Comparison of Homogeneous and Heterogeneous Fenton and Sono-Fenton Decolorization of Titan Yellow: Doehlert Optimization, Response Surface Methodology, and Synergic Effects Study

Tabaraki, Reza*+; Abedini Zahra

Department of Chemistry, Faculty of Science, Ilam University, P.O. Box 69315-516 Ilam, I.R. IRAN

ABSTRACT: *In this work, four Fenton processes were used for the decolorization of titan yellow. Experimental conditions such as concentration of H_2O_2, pH, time, zero-valent iron dose, and concentration of Fe^{2+} were optimized by Doehlert experimental design and response surface models. In the absence of ultrasonic waves, the application of zero-valent iron had an intense effect on decolorization percent (95% for heterogeneous Fenton with respect to 18% for classical Fenton). The optimum conditions were (0.0054M H_2O_2, 0.031g/L Fe^{2+}, pH 2.5 and reaction time 47 min) and (0.0013M H_2O_2, 0.194g/L zero-valent iron, pH 2.5, and reaction time 10 min) for homogeneous and heterogeneous Fenton processes, respectively. Both homogeneous and heterogeneous Sono-Fenton processes reached to decolorization percent of 100%. The optimum pH was 2.5 for the two processes. The optimum conditions for homogeneous and heterogeneous sono-Fenton processes were (0.0035M H_2O_2, 0.0037g/L Fe^{2+}, and reaction time 30 min) and (0.0014M H_2O_2, 0.4g/L zero-valent iron, and reaction time 10 min), respectively.*

KEYWORDS: *Titan Yellow; homogeneous; heterogeneous; Fenton; ultrasonic; Doehlert design.*

INTRODUCTION

Several groups of dyes (azo, anthraquinones, and xanthenes) are used in different industries. Azo dyes because of their easy and cost-effective synthesis have the most applications. Their structures have an azo group (–N=N–), aromatic rings, and sulfonic acid groups. However, they are toxic and non-degradable. Due to their good solubility, they are common water pollutants. Wastewaters containing azo dyes absorb strongly sunlight, reduce photosynthesis of aquatic plants, reduce transparency, and are responsible for different human diseases. Therefore, the removal of dyes from wastewaters has great environmental significance and commercial importance [1, 2].

Direct dyes include water-soluble azo dyes, require the presence of electrolytes for the dyeing process. They are classified as direct dyes, because they may be applied directly to celluloid fibers. Titan yellow ($C_{28}H_{19}N_5Na_2O_6S_4$, other names: Thiazole Yellow G, Clayton Yellow, C.I. Direct Yellow 9, C.I. 19540) is a direct dye extensively used in dyeing cotton, viscose rayon, natural silk. It is also used as a biological stain, analytical reagent for the determination of magnesium, fluorescent dye for microscopy, and pH indicator. Thiazole yellow G dye can cause health problems in humans after inhalation [3].

Different methods such as biosorption [4-6],

adsorption [7], ozonation [8], chemical oxidation and advanced oxidation processes [9], and different materials such as chitosan [10, 11], multiwall carbon nanotubes [12], and montmorillonite nanoparticles [13] have been used for the treatment of dyes in wastewaters. Titan yellow was removed by ultrasonic-assisted sorption on magnetic metal oxide-organic framework material [14], adsorption on polyaniline@SiO_2 nanocomposite [15], electrostatic adsorption [16], photocatalytic degradation [17,18], adsorption on maghemite nanoparticles [19], biosorption on Hypnea Musciformis powder [20], and photo‑assisted mineralization of titan yellow dye using ZnO nanorods [21].

Advanced Oxidation Processes (AOP) are efficient treatment processes in which highly reactive hydroxyl radicals are generated in-situ and react with organic pollutants. These methods have better efficiency, are easily operated, and have fewer residuals produced [22]. Fenton method, one of the important AOPs, has abundant, nontoxic, and low-cost reagents (aqueous mixtures of Fe^{2+} and H_2O_2 under acidic conditions) and has environmentally-benign of the degraded products (CO_2, water, and inorganic salts) [23]. Hydroxyl radicals are generated in the Fenton process as:

$$H_2O_2 + Fe^{2+} \rightarrow Fe^{3+} + OH^- + OH^\bullet \tag{1}$$
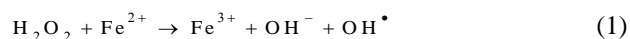
Fenton's mechanism is complex and the decomposition of H_2O_2 is catalyzed by Fe^{2+}. The Fenton reaction can take place both homogeneously and heterogeneously. In a homogeneous process, chemicals react in the entire solution. In a heterogeneous way, chemical reactions proceed on the surface of the catalyst and mass transfer limit reactants' adsorption. In Advanced Fenton Process (AFP), hydroxyl radicals are produced from metallic iron and H_2O_2 under acidic conditions. The corrosion of the iron surface also causes in situ generations of Fe^{2+}. In this process, the use of metallic iron is cheaper than iron salts and Fe^{3+} recycles faster at the iron surface [24-26].

Ultrasound can also be used for the breakup of organics of environmental concern. Sonication causes acoustic cavitation that tiny bubbles in the liquid phase are formed, grown, and collapsed. Hot spots (5000 K and 1000 atm) generated from bubbles collapse cause dissociation of water vapor in bubbles to OH radicals. These are very reactive radicals [27, 28]. Azo dyes are large, non-volatile, and hydrophilic molecules. Therefore, complete removal of these molecules is not achieved by ultrasonic waves alone [29,30].

Optimization refers to find experimental conditions for the best response. In a univariate strategy or one at a time strategy, one factor is studied at each time. In multivariate strategy, simultaneous monitoring of factors is done. Therefore, fewer experiments are needed and the study of interactions between factors is possible. In response to surface methodology (RSM), the experimental data are obtained based on experimental design. Then, a polynomial function is fitted mathematically to data. Finally, the optimum of experimental factors is determined by this mathematical model [31]. Several experimental designs such as the Central Composite Design (CCD), Box–Behnken Design (BBD), and Doehlert design are used in RSM. Doehlert design is a multilevel optimization strategy. Variables have a different number of levels and levels are assigned to variables based on their significance. Some advantages of this design are the need for fewer experiments, emphasis on uniformly space-filling, and its sequentially potential. The least attractive feature of Doehlert's design is exploring the neighboring domain by the addition of a few experiments [32].

In this work, synergic effects of ultrasonic waves and zero-valent iron in homogeneous and heterogeneous Fenton and sono-Fenton processes for decolorization of titan, yellow were compared. Experimental parameters such as Fe^{2+} or zero-valent iron dose, pH, the concentration of H_2O_2, and reaction time were optimized by a multi-level experimental design such as Doehlert design and response surface methodology.

EXPERIMENTAL SECTION
Materials and instruments
Titan yellow and sodium hydroxide, sulfuric acid, hydrogen peroxide (30%, w/w), Zero-Valent Iron (ZVI) powder (particle size 10 μm), and iron (II) sulfate heptahydrate ($FeSO_4.7H_2O$) were of analytical grade and obtained from Merck (Germany). The chemical structure of titan yellow is shown in Fig. 1. The stock dye solutions were prepared in deionized water. The pH was adjusted by sodium hydroxide or sulfuric acid using a pH meter (Metrohm, model-780, Switzerland). The final concentration of dye was determined (λ_{max}=413 nm) by a UV–Vis spectrophotometer (Varian 300 Bio, Australia). Sono-Fenton experiments were performed in an ultrasonic bath (RK103H, BANDELIN SONOREX, Germany) with a maximum capacity of 4 L (35 kHz, 140 W).
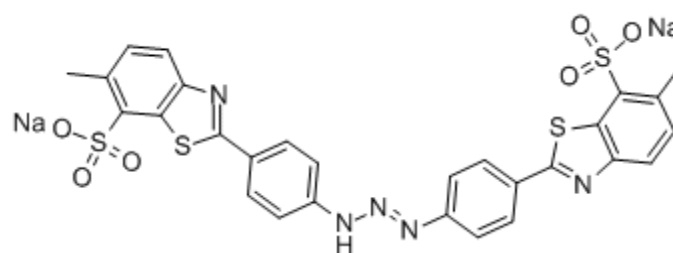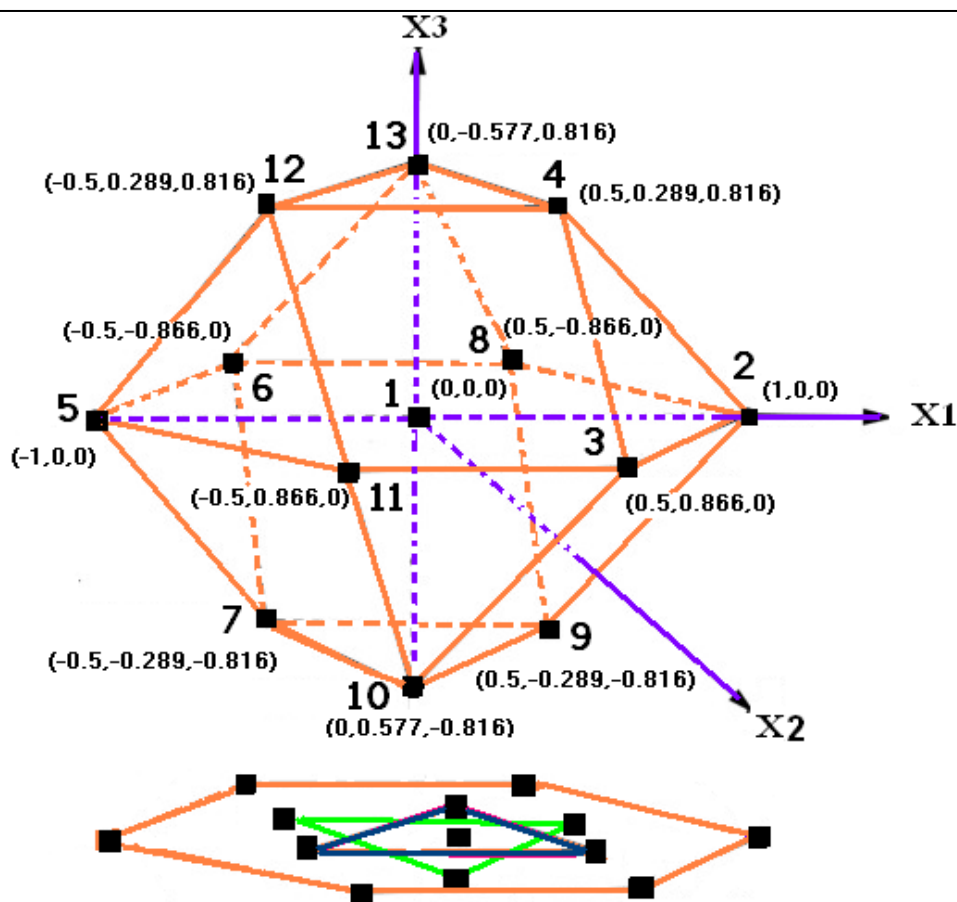
Fig. 1: Chemical structure of titan yellow.

Fig. 2: Doehlert experimental design.

Doehlert experimental design and RSM

Doehlert design with three-factor (X_1, X_2, and X_3) at different levels (7, 5, 3) was used in homogeneous and heterogeneous Fenton and sono-Fenton (Fig. 2). In experimental design, we need to determine the lowest and highest levels for each factor and in this range, design experiments are done. This range is selected based on a literature search or preliminary experiments. Doehlert design is a multilevel optimization strategy. Variables have a different number of levels and the levels are assigned to variables based on their significance. In all experiments, initial dye concentration and temperature were 3×10^{-5} M and 20 ℃, respectively.

Experimental data were fitted to the following second-order polynomial model and regression coefficients were obtained. The generalized second-order polynomial model proposed for the Response Surface Methodology (RSM) was as follows:

$$Y = \beta_0 + \sum_{i=1}^{k} \beta_i X_i + \sum_{i=1}^{k} \beta_{ii} X_i^2 + \qquad (2)$$

$$\sum_{i}^{k-1} \sum_{j}^{k} \beta_{ij} X_i X_j$$

Where b_0, b_i, b_{ii}, b_{ij} are intercept, linear, quadratic, and interaction coefficients, respectively. X_i and X_j are independent variables and k is the number of the tested variables (k = 3). The coded and real values of experimental variables are shown in Tables 1 and 2. Results were analyzed using Minitab 16 (Minitab Inc., State College, PA, USA) software.

Methods
Homogeneous Fenton and sono-Fenton processes

In homogeneous processes, the concentration of Fe^{2+} (the most significant factor, studied in 7 levels), concentration of H_2O_2 (the nest significant, studied in 5 levels), and time (studied in 3 levels) were optimized by experimental design. In homogeneous experiments, concentration of Fe^{2+}, the concentration of H_2O_2, and time were changed between 1-31 mg/L, 0.001-0.006 M, and 30-60 min, respectively. According to the preliminary studies, pH was adjusted to 2.5. In a typical experiment, dye solution (3×10^{-5} M) was added to Fe (II) solution (concentration was based on experimental design values). Sulfuric acid was used to adjust pH to 2.5. Finally, H_2O_2 solution was added based on experimental design values. The solution was mixed using a magnetic stirrer at 100 rpm rotating rate (for homogeneous Fenton) or was irradiated in an ultrasonic bath at 35 kHz and 140W (for the sono-Fenton process) at room temperature (20 ℃). Samples were withdrawn at specific time intervals during the Fenton oxidation. Time was recorded after the addition of H_2O_2 solution. The concentration of the azo dye was measured in 1cm cell by UV/Vis spectrophotometer. Removal efficiency was calculated as:

$$Removal\ efficiency(\%) = \frac{C_i - C_t}{C_i} \times 100 \qquad (3)$$

where C_i and C_t are initial and instantaneous concentrations of dye.

Heterogeneous Fenton and sono-Fenton processes

In heterogeneous processes, zero-valent iron dose (the most significant factor, studied in 7 levels), the concentration of H_2O_2 (the nest significant factor, studied in 5 levels),

and pH (studied in 3 levels) were optimized by experimental design. In heterogeneous experiments, zero-valent iron dose, the concentration of H_2O_2 and pH were changed between 0.1-0.4 g/L, 0.001-0.006 M, and 2.5-3.5, respectively. Time was set at 10 minutes according to the preliminary studies. In a typical experiment, a different amount of zero-valent iron (based on experimental design values) was added to the dye solution (3×10^{-5} M), and pH was adjusted at the desired value by sulfuric acid. Finally, H_2O_2 solution was added based on experimental design values. The solution was mixed using a magnetic stirrer at 100 rpm rotating rate (for homogeneous Fenton) or was irradiated in an ultrasonic bath at 35 kHz and 140W (for the sono-Fenton process) at room temperature (20 ℃). Samples were withdrawn after 20 minutes. Time was started after the addition of H_2O_2 solution. The concentration of the azo dye was measured in 1cm cell.

RESULTS AND DISCUSSION
Heterogeneous Fenton and sono-Fenton modeling

Zero valent iron dose, pH, and concentration of H_2O_2 were important factors and optimized by Doehlert experimental design. Zero valent iron dose (g/l) was studied at seven levels was used as the highest effective factor. Five and three levels were also used for the H_2O_2 concentration and pH, respectively. Independent variables and responses (removal %) are presented in Table 1.

Experimental data were fitted to a second-order polynomial and statistical significances were estimated by ANOVA. Second-order polynomial models for heterogeneous Fenton and sono-Fenton are shown in equations 4 and 5, respectively. Significant variables are shown as bold terms. Terms with *p*-value lower than 0.05 are considered as significant terms (confidence level: 95%).

$$Removal\% = -9.13 \times 10^{+2} - \qquad (4)$$
$$1.50 \times 10^{+4} \times [H_2O_2] - 2.90 \times 10^{+1} \times [Fe] +$$
$$7.69 \times 10^{+2} \times pH - 1.33 \times 10^{+5} \times [H_2O_2]^2 -$$
$$3.90 \times 10^{+1} \times [Fe]^2 - 1.43 \times 10^{+2} \times pH^2 +$$
$$2.80 \times 10^{+4} \times [H_2O_2] \times [Fe] +$$
$$3.20 \times 10^{+3} \times [H_2O_2] \times pH - 1.80 \times 10^{+1} \times [Fe] \times pH$$
$$R^2 = 0.999 \quad ; \quad Lack\ of\ fit = 0.196\,(p > 0.05)$$

Table 1: Doehlert experimental design for degradation of titan yellow by heterogeneous Fenton and sono-Fenton.

Exp. No.	Coded values			Real values			Removal%	
	X_1	X_2	X_3	[H_2O_2], M	Fe, g/L	pH	Fenton	Sono-Fenton
1	0	0	0	0.0035	0.25	3	85	23
2	1	0	0	0.006	0.25	3	87	0
3	0.5	0.866	0	0.00475	0.4	3	87	13
4	0.5	0.289	0.816	0.00475	0.3	3.5	10	0
5	-1	0	0	0.001	0.25	3	80	33
6	-0.5	-0.866	0	0.00225	0.1	3	90	34
7	-0.5	-0.289	-0.816	0.00225	0.2	2.5	93	90
8	0.5	-0.866	0	0.00475	0.1	3	78	43
9	0.5	-0.289	-0.816	0.00475	0.2	2.5	87	92
10	0	0.577	-0.816	0.0035	0.35	2.5	91	88
11	-0.5	0.866	0	0.00225	0.4	3	78	36
12	-0.5	0.289	0.816	0.00225	0.3	3.5	1	20
13	0	-0.577	0.816	0.0035	0.15	3.5	7	7
14	0	0	0	0.0035	0.25	3	85	25
15	0	0	0	0.0035	0.25	3	83	21

$$\mathrm{Removal\%} = 1.20 \times 10^{+3} + 2.70 \times 10^{+4} \times [H_2O_2] - \quad (5)$$

$$4.25 \times 10^{+2} \times [Fe] - 6.94 \times 10^{+2} \times pH -$$

$$1.09 \times 10^{+6} \times [H_2O_2]^2 + 4.39 \times 10^{+2} \times [Fe]^2 +$$

$$1.00 \times 10^{+2} \times pH^2 - 4.27 \times 10^{+4} \times [H_2O_2] \times [Fe] -$$

$$4.53 \times 10^{+3} \times [H_2O_2] \times pH + 1.07 \times 10^{+2} \times [Fe] \times pH$$

$$R^2 = 0.991 \quad ; \quad \mathrm{Lack\ of\ fit} = 0.054 \ (p > 0.05)$$

Where *[Fe]* is zero-valent iron dose (g/L). These models had significant linear, quadratic, and interaction terms. The coefficient of determination ($R^2 = 0.999$ and 0.991) shows the goodness-of-fit of these models and only 0.1 and 0.9% of total variance were not explained by these models. The reliability of the models was approved by the absence of any lack of fit ($p > 0.05$). The relationship between different experimental variables was graphically presented in Figs. 3A and 3B that these three-dimensional surface plots were constructed using the above equations. These response surfaces in the three-dimensional space are shown as a function of two dependent variables when the third dependent variable is kept constant at the center point.

Homogeneous Fenton and sono-Fenton modeling

The responses (removal %), coded and real values of independent variables in the experimental design are presented in Table 2. Polynomial equations of the homogeneous Fenton (equation 6) and sono-Fenton (equation 7) are as follows:

$$\mathrm{Removal\%} = -4.70 \times 10^{+1} + \quad (6)$$

$$4.00 \times 10^{+2} \times [H_2O_2] + [Fe^{2+}] + 2 \times t -$$

$$7.47 \times 10^{+5} \times [H_2O_2]^2 - 1.00 \times 10^{-4} \times [Fe^{2+}]^2 -$$

$$1.00 \times 10^{-4} \times t^2 + 2.7 \times 10^{+1} \times [H_2O_2] \times [Fe^{2+}] +$$

$$1.51 \times 10^{+2} \times [H_2O_2] \times t + 1.00 \times 10^{-4} \times [Fe^{2+}] \times t$$

$$R^2 = 0.931 \quad ; \quad \mathrm{Lack\ of\ fit} = 0.232 \ (p > 0.05)$$

$$\mathrm{Removal\%} = 1.81 \times 10^{+2} - 120 \times 10^{+4} \times [H_2O_2] - \quad (7)$$

$$3 \times [Fe^{2+}] - 2 \times t + 2.04 \times 10^{+6} \times [H_2O_2]^2 +$$

$$1.00 \times 10^{-4} \times [Fe^{2+}]^2 + 1.00 \times 10^{-4} \times t^2 -$$

$$3.2 \times 10^{+1} \times [H_2O_2] \times [Fe^{2+}] -$$

$$3.3 \times 10^{+1} \times [H_2O_2] \times t + 1.00 \times 10^{-4} \times [Fe^{2+}] \times t$$

$$R^2 = 0.931 \quad ; \quad \mathrm{Lack\ of\ fit} = 0.155 \ (p > 0.05)$$

In these models, the lack of fit is not significant

Table 2: Doehlert experimental design for degradation of titan yellow by homogeneous Fenton and sono-Fenton.

Exp. No.	Coded values			Real values			Removal%	
	X_1	X_2	X_3	$[H_2O_2]$, M	$[Fe^{2+}]$, mg/L	Time, min	Fenton	Sono-Fenton
1	0	0	0	0.0035	16	45	16	86
2	1	0	0	0.006	16	45	16	98.8
3	0.5	0.866	0	0.00475	31	45	16	100
4	0.5	0.289	0.816	0.00475	21	60	18	96.7
5	-1	0	0	0.001	16	45	6	98
6	-0.5	-0.866	0	0.00225	1	45	6	86.6
7	-0.5	-0.289	-0.816	0.00225	11	30	3	97
8	0.5	-0.866	0	0.00475	1	45	10	89
9	0.5	-0.289	-0.816	0.00475	11	30	6	99
10	0	0.577	-0.816	0.0035	26	30	10	84
11	-0.5	0.866	0	0.00225	31	45	10	100
12	-0.5	0.289	0.816	0.00225	21	60	3	98
13	0	-0.577	0.816	0.0035	6	60	4	83.6
14	0	0	0	0.0035	16	45	14	84
15	0	0	0	0.0035	16	45	17	87

(p > 0.05) and therefore regressions are reliable. Constructed three-dimensional response surface plots are shown in Figs. 3C and 3D.

Effect of process variables

Fenton-based oxidation processes are based on the generation of powerful radicals. In Fenton's mechanism, iron cycles between Fe^{2+} and Fe^{3+} oxidation states, due to reaction with H_2O_2. The oxidation of Fe^{2+} produces highly reactive hydroxyl radical (•OH), which can efficiently attack organic compounds [33-35]. Optimum conditions were obtained from RSM models. Removal percent at these conditions were shown in Table 3. As shown, the optimum pH for all of the processes was 2.5. It was suggested that the nature of wastewater has no effect on the optimal pH of the Fenton process. In many previous studies, optimal pH is around 2–4 [5].

More hydroxyl radicals generate at higher H_2O_2 doses. However, no performance improvement or even adverse effect is observed because of induced radical scavenging at high H_2O_2 concentrations. In the above RSM models, linear, quadratic, and interaction terms of H_2O_2 concentration

were significant. Effect of H_2O_2 concentration was shown in Figs. 3A-D. As shown in Table 3, H_2O_2 consumption is three times greater in the homogeneous process (0.0054 and 0.0034 M) with respect to heterogeneous processes (0.0013 and 0.0014 M).

Availability of ferrous irons determines amounts of hydroxyl radical formation and the Fenton process performance. Linear, quadratic and interaction terms of [Fe] or $[Fe^{2+}]$ were also significant in the above RSM models. Effect of the iron dose was shown in Figs. 3A-D. When Fe^{2+} concentration is very high, it scavenges the hydroxyl radicals and therefore inhibits the Fenton process. As shown in Table 3, iron consumption is greater in heterogeneous processes.

Comparison of different processes

Classical Fenton at optimum conditions reached 18% decolorization. The synergism effect of ultrasonic waves in homogeneous Fenton caused H_2O_2 and Fe^{2+} consumption to be reduced 1.5 and 9 times, respectively. In addition, the required time was reduced to 30 minutes (Table 3) and the decolorization percent reached 100%.
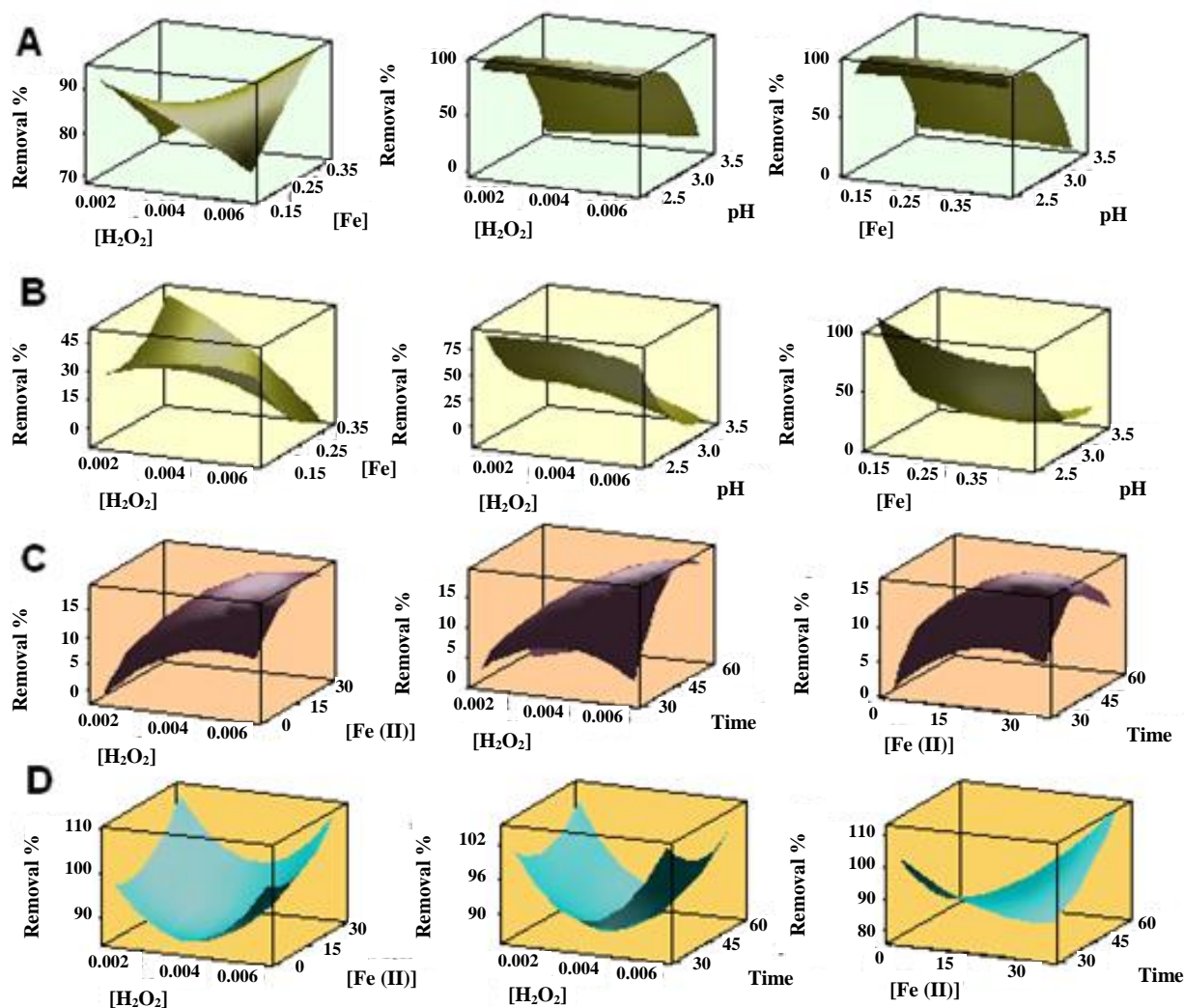
Fig. 3: Response surface plots of A) heterogeneous Fenton, B) heterogeneous sono-Fenton, C) homogeneous Fenton and D) homogeneous sono-Fenton processes of titan yellow removal.

In heterogeneous processes, pH, time, and $[H_2O_2]$ were similar (Table 3) but again positive synergism effect of ultrasonic waves improved decolorization percent from 95% to 100%. The synergistic effect is generally attributed to an increase of OH radical concentration by ultrasound.

In the absence of ultrasonic waves, the application of zero-valent iron (heterogeneous Fenton) had an intense effect on decolorization percent (18% → 95%) with respect to classical Fenton (use of Fe^{2+}). Although, in this process, iron consumption was the higher lower oxidant was used and decolorization time was reduced from 47 to 10 minutes (Table 3).

Both homogeneous and heterogeneous sono-Fenton processes reached to decolorization percent of 100% (Table 3). The optimum pH was 2.5 for the two processes.

In the homogeneous sono-Fenton process, iron consumption is lower but the decolorization time is 30 minutes but in the heterogeneous sono-Fenton process, H_2O_2 consumption is lower and the decolorization time is 10 minutes.

The economic aspect of the process is a very important factor for the selection of a system. Based on the costs of industrial chemicals (zero-valent iron, 1$/kg; $FeSO_4.7H_2O$, 1$/Kg; H_2O_2 35%, 0.34$/Kg) and 1m³ of wastewater containing 3×10^{-5} M of titan yellow, the total cost of chemicals was evaluated for the homogeneous Fenton (0.27$), homogeneous sono-Fenton (0.09$), heterogeneous Fenton (0.05$), and heterogeneous sono-Fenton (0.43$) processes. As shown in Table 3, the heterogeneous Fenton reaches 95% removal at 10 min and does not require the ultrasonic device and is fast and the

Table 3: Optimized conditions for homogeneous and heterogeneous Fenton and sono-Fenton processes.

variable	Homogeneous		Heterogeneous	
	Fenton	sono-Fenton	Fenton	sono-Fenton
[H$_2$O$_2$], M	0.0054	0.0035	0.0013	0.0014
[Fe(II)], [Fe], g/L	0.031	0.0037	0.194	0.4
Time (min)	47	30	10	10
pH	2.5	2.5	2.5	2.5
Removal%	18.2	100	95	100

most economical process. If the goal is 100% removal, heterogeneous sono-Fenton (time: 10 min) is preferable to homogeneous sono-Fenton process (time: 30 min) because electrical power consumption is three times.

CONCLUSIONS

In this work, four Fenton processes such as homogeneous Fenton, homogeneous sono-Fenton, heterogeneous Fenton, and heterogeneous sono-Fenton were used for decolorization of titan yellow. Experimental conditions such as H$_2$O$_2$ concentration, pH, time, zero-valent iron dose and

Fe^{2+} concentrations were optimized by Doehlert experimental design and response surface models.

Acknowledgment

REFERENCES

[1] Fernández C., Larrechi M.S., Callao M. P., An Analytical Overview of Processes for Removing Organic Dyes from Wastewater Effluents, *TrAC Trend. Anal. Chem.*, **29(10)**: 1202-1211 (2010).

[2] Wang N., Zheng T., Zhang G., Wang P., Degradation of Reactive Brilliant Red in Aqueous Solution by Ultrasonic Cavitation, *Ultrason. Sonochem.*, **15(1)**: 43-48 (2008).

[3] Bankole P.O., Adekunle A.A., Govindwar S.P., Demethylation and Desulfonation of Textile Industry dye, Thiazole Yellow G by *Aspergillus niger* LAG, *Biotechnol. Report.,* **23**: e00327 (2019).

[4] Tabaraki R., Sadeghinejad N., Biosorption of Six Basic and Acidic Dyes on Brown Alga Sargassum Ilicifolium: Optimization, Kinetic and Isotherm Studies, *Water Sci. Technol.*, **75(11)**: 2631–2638 (2017).

[5] Tabaraki R., Khodabakhshi M., Multidye Biosorption: Wavelet Neural Network Modeling and Taguchi L$_{16}$ Orthogonal Array Design, *Clean-Soil Air Water*, **45(5)**: 1500499 (2017).

[6] Tabaraki R., Heidarizadi E., Simultaneous Multidye Biosorption by Chemically Modified *Sargassum glaucescens*: Doehlert Optimization and Kinetic, Equilibrium, ad Thermodynamic Study in Ternary System, *Separ. Sci. Technol.*, **52(4)**: 583-595 (2017).

[7] Naghizadeh A., Nabizadeh R., Removal of Reactive Blue 29 Dye by Adsorption on Modified Chitosan in the Presence of Hydrogen Peroxide, *Environm. Prot. Eng.*, **42(1)**: 149-168 (2016).

[8] Malik S.N., Ghosh P.C., Vaidya A.N., Mudliar S.N., Hybrid Ozonation Process for Industrial Wastewater Treatment: Principles and Applications: A Review, *J. Water Process Eng.*, **35**: 101193 (2020).

[9] Nidheesh P.V., Gandhimathi R., Ramesh S.T., Degradation of Dyes from Aqueous Solution by Fenton Processes: A Review, *Environ. Sci. Pollut. Res.*, **20**: 2099-2132 (2013).

[10] Naghizadeh A., Ghafouri M., Synthesis and Performance Evaluation of Chitosan Prepared from Persian Gulf Shrimp Shell in Removal of Reactive Blue 29 Dye from Aqueous Solution (Isotherm, Thermodynamic and Kinetic Study), *Iran. J. Chem. Chem. Eng. (IJCCE)*, **36(3)**: 25-36 (2017).

[11] Tabaraki R., Sadeghinejad N., Comparison of Magnetic Fe$_3$O$_4$/chitosan and Arginine-Modified Magnetic Fe$_3$O$_4$/Chitosan Nanoparticles in Simultaneous Multidye Removal: Experimental Design and Multicomponent Analysis, *Int. J. Biol. Macromol.*, **120:** 2313-2323 (2018).

[12] Dehghani M.H., Naghizadeh A., Rashidi A., Derakhshani E., Adsorption of Reactive Blue 29 Dye from Aqueous Solution by Multiwall Carbon Nanotubes, *Desalin. Water Treat.*, **51(40-42)**: 7655-7662 (2013).

[13] Kamranifar M., Naghizadeh A., Montmorillonite Nanoparticles In Removal of Textile Dyes from Aqueous Solutions: Study of Kinetics and Thermodynamics, *Iran. J. Chem. Chem. Eng (IJCCE).*, **36(6)**: 127-137 (2017).

[14] Elwakeel K.Z., Shahat A., Khan Z.A., Alshitari W., Guibal E., Magnetic Metal Oxide-Organic Framework Material for Ultrasonic-Assisted Sorption of Titan Yellow and Rose Bengal from Aqueous Solutions, *Chem. Eng. J.*, **392(15)**:123635 (2020).

[15] Rastgordani M., Zolgharnein J., Mahadavi V., Derivative Spectrophotometry and Multivariate Optimization For Simultaneous Removal of Titan Yellow and Bromophenol Blue Dyes Using Polyaniline@SiO$_2$ Nanocomposite, *Microchem. J.,* **155**:104717 (2020).

[16] Cheng M., Li N., Zhu M., Zhang L., Deng Y., Deng C., Positively Charged Microporous Ceramic Membrane for the Removal of Titan Yellow Through Electrostatic Adsorption, *J. Environm. Sci.*, **44**: 204-212 (2016).

[17] Shilpa Hiremath M.A.L., Antony Raj M.N., Chandra Prabha V.C., *Tamarindus indica* Mediated Biosynthesis of Nano TiO$_2$ and its Application in Photocatalytic Degradation of Titan Yellow, *J. Environm. Chem. Eng.,* **6(6):** 7338-7346 (2018).

[18] Pal S., Mondal S., Maity J., Mukherjee R., Synthesis and Characterization of ZnO Nanoparticles Using Moringa Oleifera Leaf Extract: Investigation of Photocatalytic and Antibacterial Activity, *Int. J. Nanosci. Nanotechnol.*, **14(2)**: 111-119 (2018).

[19] Akrami A., Niazi A., Synthesis of Maghemite Nanoparticles and its Application for Removal of Titan Yellow from Aqueous Solutions Using Full Factorial Design, *Desalin. Water Treat.*, **57(47)**:1-14 (2016).

[20] Raju Ch. A. I., Sunil K., Studies on Biosorption of Titan Yellow Dye With Hypnea Musciformis Powder and Optimization Through Central Composite Design, *Int. J. Innov. Res. Sci. Technol.*, **5(1)**: 2349-6010 (2018).

[21] Vidya1 C., Manjunatha C., Sudeep M., Ashoka S., Lourdu Antony Raj M.A., Photo-Assisted Mineralisation of Titan Yellow Dye Using ZnO Nanorods Synthesised Via Environmental Benign Route, *SN Appl. Sci.*, **2**: 743 (2020).

[22] Ribeiro A.R., Nunes O.C., Pereira M.F.R., Silva A.M.T., An Overview on the Advanced Oxidation Processes Applied for the Treatment of Water Pollutants Defined in the Recently Launched Directive 2013/39/EU. *Environ. Int.*, **75:** 33-51 (2015).

[23] Wang J.L., Xu L.J., Advanced Oxidation Processes for Wastewater Treatment: Formation of Hydroxyl Radical and Application, *Crit. Rev. Environ. Sci. Tec.*, **42**:251-325 (2012).

[24] Von Sonntag C., Advanced Oxidation Processes: Mechanistic Aspects, *Water Sci. Technol.*, **58(5)**: 1015-1021 (2008).

[25] Guan X., Sun Y., Qin H., Li J., Lo I.M.C., He D., Dong H., The limitations of Applying Zero-Valent Iron Technology in Contaminants Sequestration and the Corresponding Countermeasures: the Development In Zero-Valent Iron Technology in the Last Two Decades (1994–2014), *Water Res.*, **75(15)**: 224-248 (2015).

[26] Khaloo S.S., Zolfaghari H., Gholamnia R., Response Surface Methodology for Optimization of 4-Nitrophenol Degradationby a Heterogeneous Fenton-like Reaction on Nano-Zero-Valent Iron, *Desalin. Water Treat.*, **56(8)**: 2206-2213 (2015).

[27] Ince N.H., Ultrasound-Assisted Advanced Oxidation Processes for Water Decontamination, *Ultrason. Sonochem.*, **40**: 97-103 (2018).

[28] Bagal M.V., Gogate P.R., Wastewater Treatment Using Hybrid Treatment Schemes Based on Cavitation and Fenton Chemistry: A Review, *Ultrason. Sonochem.*, **21(1):** 1-14 (2014).

[29] Cai M., Su J., Lian G., Wei X., Dong C., Zhang H., Jin M., Wei Z., Sono-Advanced Fenton Decolorization of Azo Dye Orange G: Analysis of Synergistic Effect and Mechanisms, *Ultrason. Sonochem.*, **31**:193-200 (2016).

[30] Siddique M., Farooq R., Price G.J., Synergistic Effects of Combining Ultrasound with the Fenton Process in the Degradation of Reactive Blue 19, *Ultrason. Sonochem.*, **21(3)**: 1206-1212 (2014).

[31] Nair A.T., Makwana A.R., Ahammed M.M., The Use of Response Surface Methodology For Modeling and Analysis of Water and Wastewater Treatment Processes: A Review, *Water Sci. Technol.*, **69(3)**: 464-478 (2014).

[32] Ferreira S.L.C., dos Santos W.N.L., Quintella C.M., Neto B.B., Bosque-Sendra J.M., Doehlert Matrix: A Chemometric Tool for Analytical Chemistry, Review, *Talanta*, **63(4)**: 1061-1067 (2004).

[33] Naghizadeh A., Regeneration of Carbon Nanotubes Exhausted with Humic Acid Using Electro-Fenton Technology, *Arab. J. Sci. Eng.,* **41(1)**: 155-161 (2016).

[34] Naghizadeh A., Nasseri S., Mahvi A.H., Rashidi A., Nabizadeh R., Rezaei Kalantary R., Fenton Regeneration of Humic Acid-Spent Carbon Nanotubes, *Desalin. Water Treat.*, **54(9)**: 2490-2495 (2015).

[35] Naghizadeh A., Momeni F., Derakhshani E., Efficiency of Ultrasonic Process in Regeneration of Graphene Nanoparticles Saturated with Humic Acid, *Desalin. Water Treat.*, **70**: 290-293 (2017).

Research Article